Steel and Composite Structures, *Vol. 34, No. 6* (*2020*) *863-875*
DOI: https://doi.org/10.12989/scs.2020.34.6.863

Experimental and numerical evaluation of rigid connection with reduced depth section

Allah Reza Moradi Garoosi[1a], Mehrzad Tahamouli Roudsari[*2] and Behrokh Hosseini Hashemi[3b]

[1]*Department of Civil Engineering, Sanandaj Branch, Islamic Azad University, Sanandaj, Iran*
[2]*Department of Civil Engineering, Kermanshah Branch, Islamic Azad University, Kermanshah, Iran*
[3]*Structural Eng. Research Center, The Int'l Institute of Earthquake Engineering and Seismology (IIEES), Tehran, Iran*

(*Received March 28, 2019, Revised January 23, 2020, Accepted February 18, 2020*)

Abstract. After medium or strong earthquakes, damage in the reduced portion of RBS connections occurs due to plastic deformations. The purpose of this paper is to numerically and experimentally investigate the reduced depth section connection as a replaceable fuse. In this regard, three commonly used rigid connections with RBS, a replaceable fuse with RBS, and a replaceable fuse with Reduced Depth Section (RDS-F) were evaluated. All specimens were subjected to quasi-static cyclic load until failure. Although the final strength of the RDS-F is lower than that of the other two, laboratory results showed that it had the maximum ductility among the three samples. The numerical models of all three laboratory samples were constructed in ABAQUS, and the results were verified with great accuracy. The results of more than 28 numerical analyses showed that the RDS-F sample is more ductile than the other specimens. Moreover, the thickness of the web and the plastic section modulus increasing, the final strength would be equal to the other specimens. Therefore, the modified RDS-F with replaceability after an earthquake can be a better alternative for RBS connections.

Keywords: steel moment resisting frame; rigid connection; replaceable fuse; beam with reduced depth section; beam with reduced flange section

1. Introduction

Brittle failure in connections is one of the most destructive types of failure. It can prevent the structure from reaching its final performance. The widespread failure of steel rigid connections in Northridge and Kobe earthquakes encountered common rigid connections of that time with a big question. Extensive research on rigid connections with complete penetrating groove weld showed that there was probability of a brittle and early failure in the welds in low drift (Engelhardt and Husain 1993, Miller 1998, Mahin 1998). One of the proposed solutions to improve the performance of these types of connections after the Northridge earthquake was the use of connections with Reduced Beam Section (RBS). In this type of connection, the reduction of the beam flange section causes the plastic hinge to be transported into the beam and, like a fuse, prevent failure in the panel zone. RBS connections, which are one of the pre-qualified rigid connections (ANSI/AISC 358–16 2016), have been widely tested. It provides a suitable energy dissipation and ductility under cyclic loading. However, the limitation of this plan is the severe non-elastic deformations in the reduced area. This makes it inevitable to replace the beam after a moderate or strong earthquake. It is very difficult, if not impossible, to replace the beams due to the connection of the roof joists to the girders.

In case of RBS connections, while comparing their performance with the common beams, extensive researches have been conducted (Sofias *et al.* 2014, Swati and Gaurang 2014, Oh *et al.* 2015). The results showed that RBS connections are an effective step in maintaining the connection and preventing brittle failure. The researchers tried to improve the performance of the connection by adding stiffener plates in the web of the reduced section (Deylami and Tabar 2013, Roudsari *et al.* 2015, TahamouliRoudsari *et al.* 2016). These stiffeners increased the ductility by delaying the local buckling in the reduced cross-sectional area. Researchers continued laboratory and numerical studies on bolted and welded RBS connections on the reconsideration of the cut geometry provisions in the flange, web, and the specification and type of the end plate (Hedayat and and Celikag 2009, Hassanien *et al*. 2014, Tsavdaridis and Papadopoulos 2016, Maleki and Tabbakhha 2012, Rahnavard *et al*. 2015, Tsavdaridis *et al*. 2014). Their studies showed that the appropriate selection of the dimensions of the end plate, geometry, and reduced cross-section dimensions could improve ductility and seismic performance of the moment resistant frame. This could also assist in transferring the plastic hinge area out of connection.

In other study, the seismic performance of rigid skewed beam-to-column connection with reduced beam section was

∗Corresponding author, Associate Professor
E-mail: atahamouli@iauksh.ac.ir
[a] Ph.D.
[b] Associate Professor

Copyright © 2020 Techno-Press, Ltd.
http://www.techno-press.org/?journal=scs&subpage=6 ISSN: 1229-9367 (Print), 1598-6233 (Online)

investigated (Zareia *et al.* 2016). The results showed that using a balanced and strong panel zone would be the best choice for a suitable performance and a higher energy absorption in this connection. The performance of a novel weak-axis reduced beam section connection under the influence of cyclic loading was investigated (Lu *et al.* 2018). In that study, in addition to the proposition of a design method for this type of connection based on experimental and numerical results, it was demonstrated that the influence of components of the connection is quite significant on its overall behavior. Numerous investigations on different types of tubular web reduced beam section connections have shown that compared to the conventional RBS, the occurrence of lateral torsional buckling in these connections is delayed (Saleh *et al.* 2016, Zahrai *et al.* 2017a, Zahrai *et al.* 2017b). Additionally, this type of connection increases energy dissipation and its story drift capacity is greater than what is required by seismic design codes. Also, due to the arch-like shape of the tubular section, the distribution of strain is better than the sharp-edged accordion web. In other study, the effects of the local buckling of the web on the cyclic behavior of reduced web beam sections were evaluated (Akrami and Erfani 2015). The results showed that in this connection, the local buckling of the web in the areas close to the hole plays an important role in the cyclic behavior of the connection.

In 2006, Wilkinson *et al.* investigated a type of RBS connection with a decrease in web height. Their suggested sample had a height drop in the web—like a wedge on one side of the beam—and a fairly good performance. In the hysteresis diagram, the pinching effect was clearly evident, which was considered to be a weakness in the connection. The researchers, with a decrease in flange and web cross-section area, were able to transfer the location of the plastic hinge to an area outside the panel zone. It not only provided proper ductility, but also minimized the damage to the panel zone. However, due to the stress concentration in the reduced area after moderate or strong earthquakes, the beam must be repaired or replaced, which, if not impossible, would be very difficult and costly.

The main objective of this paper is to numerically and experimentally investigate the use of the depth reduced cross-section, which can be used as a replaceable fuse. For this purpose, three full-scale laboratory samples of IPB equivalent wide flange section were made. The samples were subjected to quasi-static and cyclic loading up to a drift of about 9%. The first one was the RBS and the end plate. In the second and third samples, it was tried to use a short replaceable fuse at the end of the beam and place the reduced cross-section in the fuse part. Thus, the second specimen consisted of a fuse of 35.5cm in length and a beam with reduced section in the flange. In fact, in the second sample, the Reduced Beam Section was used as a Fuse (RBS-F). In the third sample, the Reduced Depth Section was also used as a Fuse (RDS-F). Similar to the second sample, the length of the fuse in the third sample was chosen to be 35.5 cm.

Based on the experimental results, the hysteresis, backbone, and equivalent bilinear diagrams were plotted for all specimens. Moreover, the seismic parameters of the samples were evaluated and compared. The results showed that the RBS-F and RDS-F samples exhibited a more suitable performance than the first specimen and could be used as a replaceable fuse in steel moment resistant frames. However, the ultimate strength drop in RDS-F was significant. For more precise examination, numerical modeling and nonlinear finite element analysis were used.

According to the laboratory data, the numerical model of all the three samples was verified with high accuracy. Then for 28 numerical models, the hysteresis, backbone, and the equivalent bilinear diagrams were plotted and calculation of ductility, energy dissipation, and equivalent stiffness were done. Based on experimental and numerical samples, a Reformed type of Fuse was provided with an RDS connection (RDS-FR). The final results showed that the RDS-FR sample was not only more ductile than the RBS and RBS-F specimens, but also had an appropriate strength and stiffness.

2. Sample specifications and test setup

After the experience of the Northridge earthquake, two strategies were adopted to prevent the failure of rigid connections in steel structures: strengthening the connection or weakening the beam at a location close to the connection. In this study, both strategies have been simultaneously employed. This was done to not only concentrate the damage in the fuse, but also to protect the area where the fuse was connected to the column from damage. Such a strategy would increase the feasibility of replacing the fuse after the occurrence of an earthquake.

The samples were assembled at the NOVIN SAZE FIDER ZAGROSS Company and tests were carried out at the structural research lab of Islamic Azad University of Kermanshah. The research was carried out on three full-scale specimens with an equivalent IPB cross-section made of steel plates of ST37 nominal rating, with nominal yield stress and modulus of elasticity equal to 240 MPa and 200 GPa, respectively. For connecting the end plate of the beam to the column, bolts with a diameter of 24mm and H.R. 10.9 were used (ISO 898-1 2009).

In all the three samples, the length of the column was 2000 mm and the length of the beam was 1445mm (from the centerline of the column to the point where the load is applied). The behavior of a connection can be affected by the capacity of the column, beam, and panel zone. According to the purpose of the study—which was to evaluate the performance of the RDS and RBS fuse—a stronger column and a panel zone were used in order to fully form the plastic hinge in the beam (Lee et al. 2005). The sectional dimensions of the beam and column are presented in Table 1.

Table 1 Dimensions of the column and the beam

	Flange (mm)	Web (mm)
Beam	180×15	150×8
Column	240×20	200×10

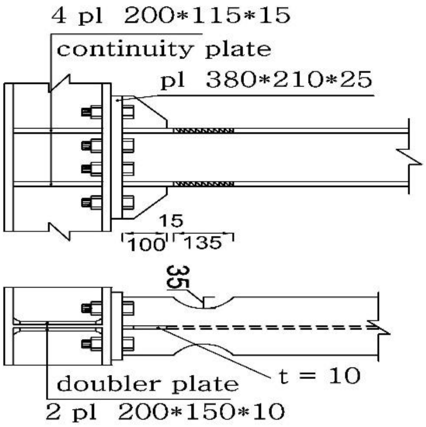

Fig. 1 The RBS sample

The first sample is shown in Fig. 1 with a reduced cross-section and a stiffened end-plate. The dimensions and cutting geometry were selected according to the instructions enumerated in the AISC code (ANSI/AISC 358–16 2016). In samples 2 and 3, a short connector was used as a replaceable fuse. The connection of these components to the beam and column was carried out through the end plates and bolts (Fig. 2).

In specimen 2, a common reduced flange section was used as the first specimen. The possibility of lateral-torsional buckling increased by reducing the flange width. Therefore, in third sample, the beam's height in the fuse area was reduced without changing the dimensions of the beam's flange in such a way that its plastic section modulus stood almost equal to sample 2. This was done in order to improve the performance in the third specimen with a change in the geometry of the reduced cross-section. The RDS-F sample crescents were created in cold rolling, which resulted in significant residual stresses. In both the samples 2 and 3, a seating on the column was used for two objectives: strengthening of the panel zone and convenient replacement of the fuse after possible earthquake damage. The complete penetrating groove weld was used to connect the beam and the fuse to the end plates, and fillet welding was used in the remaining cases. The SMAW process was applied for the weldings and the quality of the welds was controlled and approved via non-destructive testing.

As shown in Fig. 3, a strong chassis was used to arrange the tests in the laboratory and proper supports for columns. In this arrangement, the column was placed horizontally and the beam was mounted vertically with the help of eight bolts of 24 mm diameter and H.R. 10.9 in the column. All bolt connections were of friction type, and the bolts were completely pre-stressed. The required pre-stressing force for a bolt with the diameter of 24 mm is equal to 220 kN, which is equivalent of an 800 N.m torque (DIN 1990). As shown in Fig. 3, a hydraulic actuator with a minimum capacity of 1000 kN and maximum stroke of 300 mm was used to apply quasi-static cyclic loading. The centerline height of the point where the jack is connected to the beam, from the end plate was 1300 mm in the first specimen, and 1150 mm in the second and third samples due to the presence of a seating. Meanwhile, an appropriate structure was used to the lateral bracing of the beam.

Linear Potentiometer Transducers (LPTs), with the appropriate stroke were used to measure the displacements of the end and middle of the beam, the rotation of the panel zone, and the separation of the endplate. The LPTs had a precision of 0.01 to 0.04 mm. Moreover, a load cell placed between the actuator and the specimens was used to measure the applied force.

Tensile test was performed based on the ASTM standard in order to examine the materials used in the beam, column, endplates, stiffeners, and bolts (ASTM Standard A370-02 2002). The modulus of elasticity, yield stress, ultimate stress, and material failure strain were also obtained. The results are presented in Table 2.

The samples were subjected to cyclic loading as per the FEMA loading protocol (FEMA- 350 2000). The number of loading cycles and corresponding drifts are shown in Table 3 and Fig. 4. The values of drifts were multiplied at the corresponding height of the beam and applied on its top as displacement. The loading continued, so that the beam fails and the hysteresis diagram would be declined. The samples were constructed with as much care and attention as possible to make the conduction of additional tests unnecessary. Therefore, when the samples were being built, extreme attention was placed on different aspects such as the dimensions, the quality of the steel, the quality of the weldings, etc.

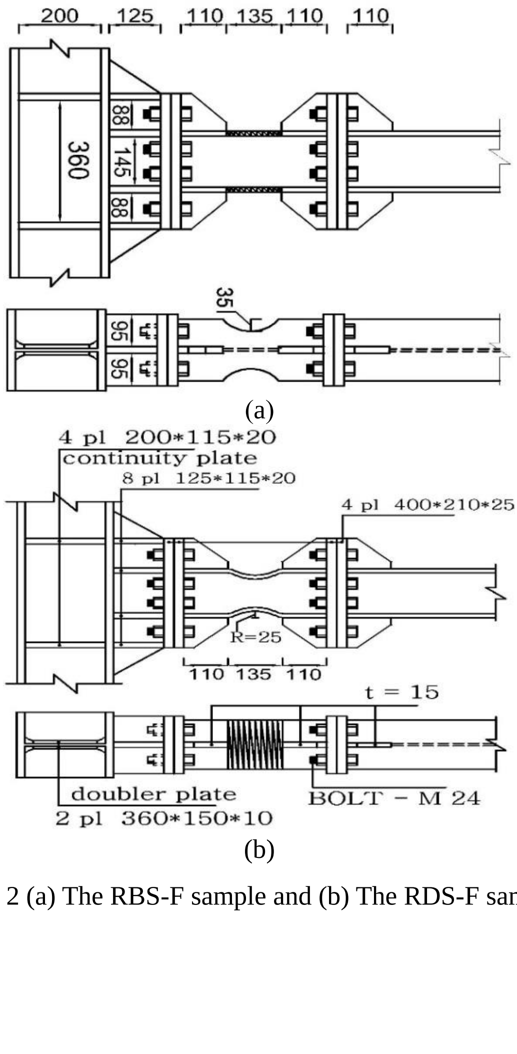

Fig. 2 (a) The RBS-F sample and (b) The RDS-F sample

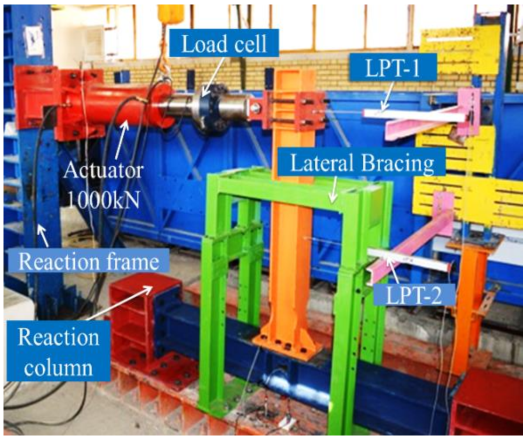

(a)

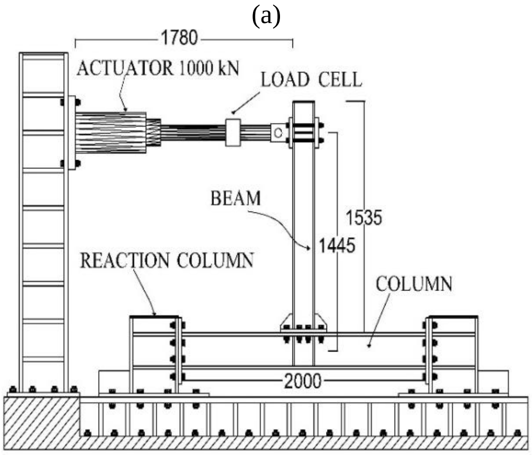

(b)

Fig. 3 (a) The RBS sample and (b) Schematic view of test setup

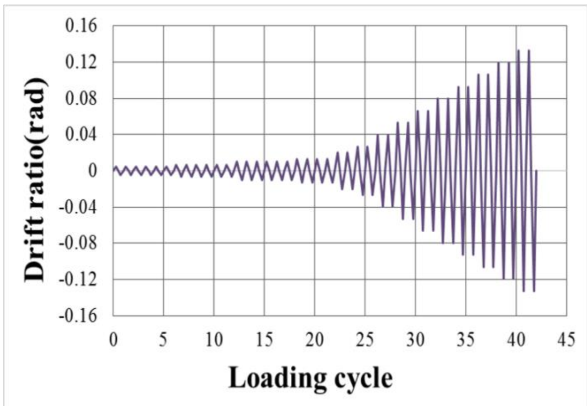

Fig. 4 The loading protocol

Table 2 Tensile tests results of the samples

Plate thickness (mm)	Elasticity modulus (GPa)	Yield stress (MPa)	Ultimate stress (MPa)	Failure strain
25	193.5	329.0	417.7	20.4
20	197.2	355.1	411.9	25.8
15	195.6	350.2	451.0	18.8
10	189.2	268.8	430.1	26.2
8	191.7	240.1	372.1	29.8
Bolt	211.1	821.6	1046.6	13.0

Table 3 Loading protocol and cycles

Number of cycles	Drift (rad)
6	0.00375
6	0.005
6	0.0075
4	0.01
2	0.015
2	0.02
2	0.03
2	0.04

Continue loading at increments of θ=0.01 rad, with two cycles of loading at each step.

3. Test Results and validation of numerical models

All the three samples were subjected to cyclic loading in the lab and moment-drift diagrams were obtained. The moment in each sample was obtained by multiplying the force of the actuator by the beam's height (until the surface of the endplate). Furthermore, numerical analyses were performed using the ABAQUS (2016) finite element software with nonlinear geometry and material considerations. Eight-node solid elements with the reduced integration (C3D8R) were used for modelling. In the finite element models, the contact between the surfaces was furnished via the "hard contact" and "Penalty" models, with the friction coefficient of 0.33. The analysis was done using the "Static General" solver and the nonlinear and hardening behaviors of the material are accounted for using the "von Mises" criterion and "combine" model, respectively. Moreover, the characteristics of the materials, presented in Table 2, were used for the materials of the column, beam, end plate, stiffeners, doubler plates, continuity plates, seating plates, and bolts. Support conditions and loading of numerical models were considered exactly in accordance with the laboratory samples.

In the numerical model, the bolts were first pre-stressed up to the required amount. Then, a lateral cyclic displacement was applied to the beam. The results of hysteresis curves in numerical models were in good agreement with the laboratory samples, and showed that the results of numerical models were reliable for the assessment and analysis of other sections. Furthermore, laboratory observations of the stages of failure formation, and comparison of laboratory results and numerical analyses were presented for all the samples.

3.1 RBS sample

Due to the proper performance of the connection, nothing happened to the connection and beam components in the laboratory before the drift of 0.08. Cracks were seen at the drift of 0.08 at the connection point of the web to the flange, as well as in the middle of the flange crescent cutting (Fig. 5(a)). With the development of the crack in the flange of the beam and its propagation to the web, the moment-drift diagram dropped rapidly at 0.09 drift and the connection was destroyed (Fig.

5(b)). A comparison of moment-drift hysteresis diagram in the laboratory sample and the numerical model is presented in Fig. 6. The hysteresis diagram of the connection was suitable, and the numerical and laboratory results were in very good agreement in terms of moment and stiffness. Fig. 7 shows the RBS sample at the end of loading in the numerical model. Most plastic strains were formed at the reduced cross-section, and the welds and panel zones were adequately protected against damage. This sample had a very good performance, but its only weakness was irreplaceability after the earthquake.

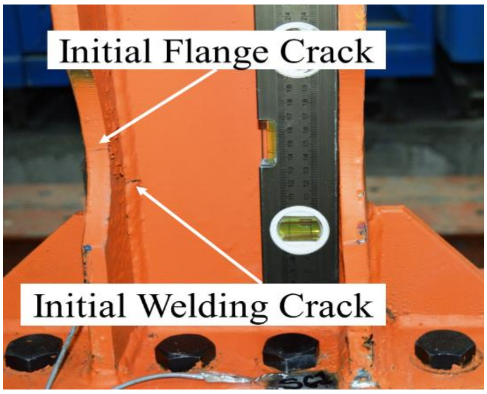

(a)

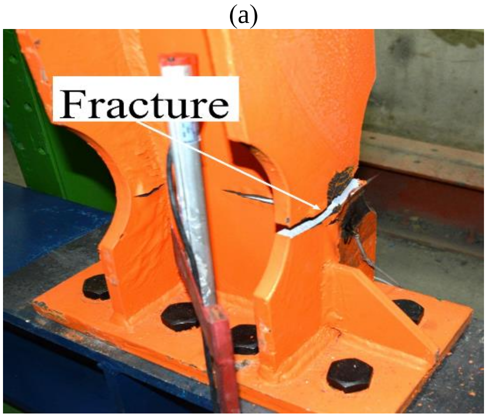

(b)

Fig. 5 (a) Crack initiation and (b) failure in the flange and the web of the beam

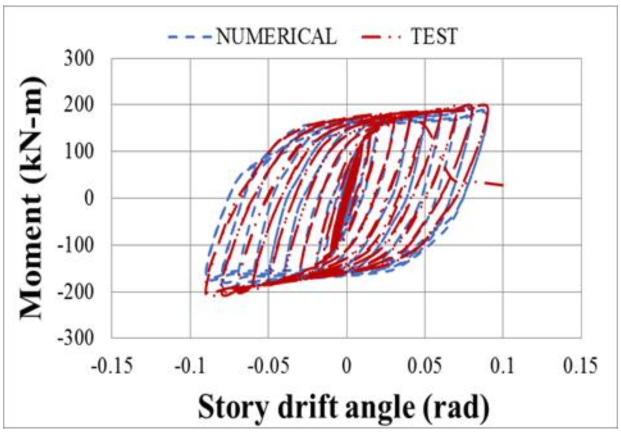

Fig. 6 Experimental and numerical moment-drift diagram for RBS sample

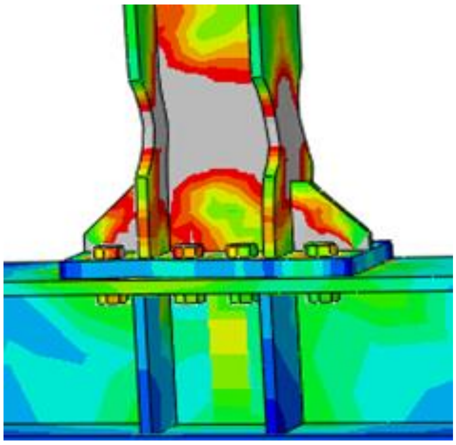

Fig. 7 Final von Mises stress distribution in the RBS Sample in the numerical model

3.2 RBS-F sample

There was no specific failure in the connection and beam components up to the drift of 0.07 in this sample. In the second cycle of the drift of 0.07, cracking and buckling began at the flange (Fig. 8(a)). Eventually, the connection failed in the drift of 0.08 with a tear in the flange (Fig. 8(b)). Moment-drift diagram of the experimental and numerical samples are presented in Fig. 9. Fig. 10 shows the von Mises stresses at the end of loading in the numerical model. The connection performance for the type of failure and hysteresis diagram was very similar to that of the RBS sample. However, the RBS-F sample was superior as far as the replaceability of the fuse after the damage was concerned.

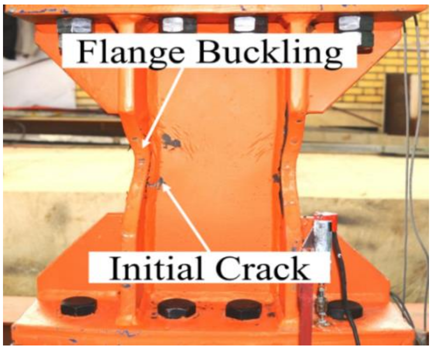

(a)

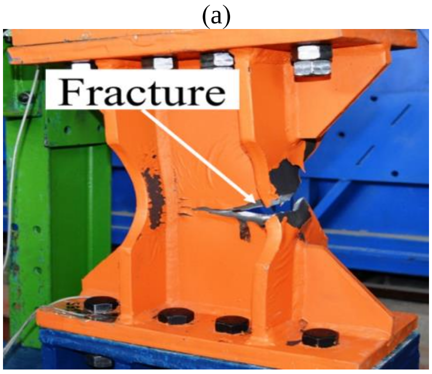

(b)

Fig. 8 (a) Buckling and crack initiation in the flange and (b) Failure in the flange and the web of the beam

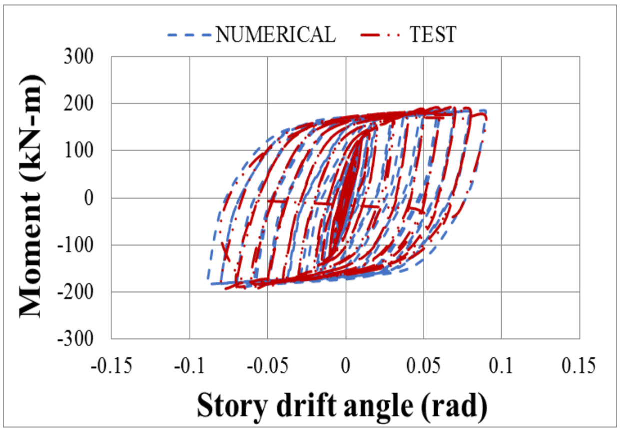

Fig. 9 The experimental and numerical moment-drift diagram of the RBS-F sample

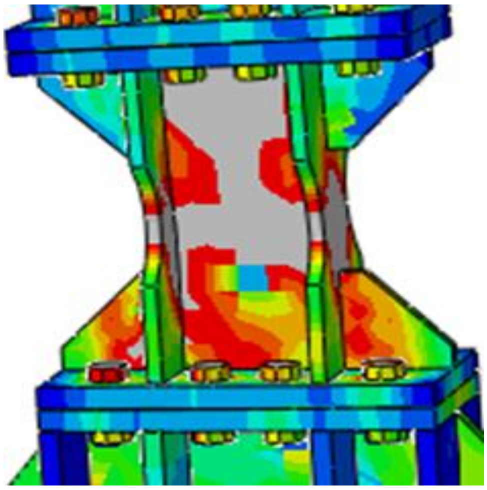

Fig. 10 Final von Mises stress distribution in the RBS-F sample in the numerical model

3.3 RDS-F sample

Failure was not observed in the components of the connection up to the 0.08 drift in this sample. Cracking began as there was continued loading at the connection of the web to the flange. As shown in Fig. 11(a), the crack and fracture propagated to the web in the drift of 0.09. With the tear of the web and the beginning of the crack in the flange of the beam, the flange was ruptured in 11% drift (Fig. 11(b)). Interestingly, the type of failure in this specimen differed from the two previous ones, and the rupture began from the web. The reason for this is discussed in the final part of the paper. As shown in Fig. 12, the hysteresis diagram of this sample shows its high-rotational capacity. Therefore, it was expected that this sample would have a higher ductility than the first and second samples. Fig. 13 shows the von Mises stress distribution at the end of the loading. Moreover, the highest stress was observed in the reduced area, which maintains the panel zone.

The final strengths of the RBS, RBS-F, and RDS-F samples were 190.54, 185.16, and 104.02kN.m respectively.

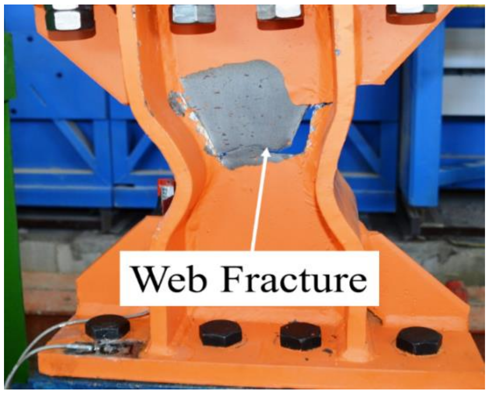

(a)

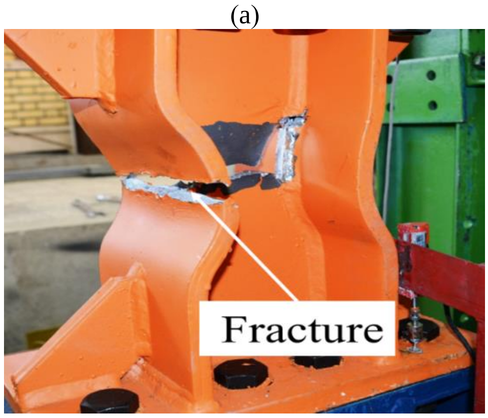

(b)

Fig. 11 (a) Crack and fracture in the web and (b) failure in the flange and the web of the beam

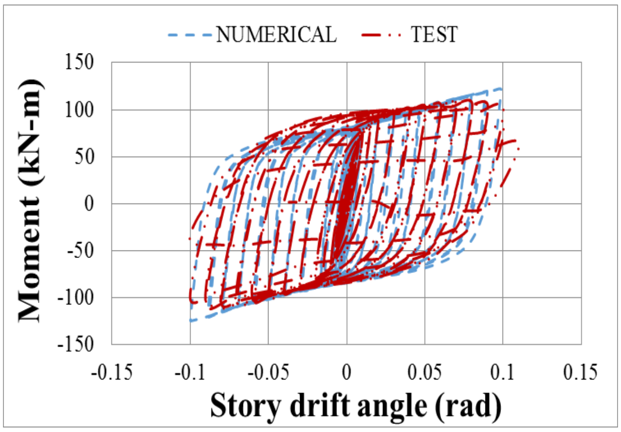

Fig. 12 The experimental and numerical moment-drift diagram of the RDS-F sample

Therefore, the extreme strength reduction of the RDS-F sample compared to other samples can be considered as its weakness. The following sections discuss the investigation and elimination of this weakness in detail.

4. Numerical Studies

In this section, a nonlinear finite element analysis was used in order to perform a better comparison among the behavior of the samples. The specifications of the numerical

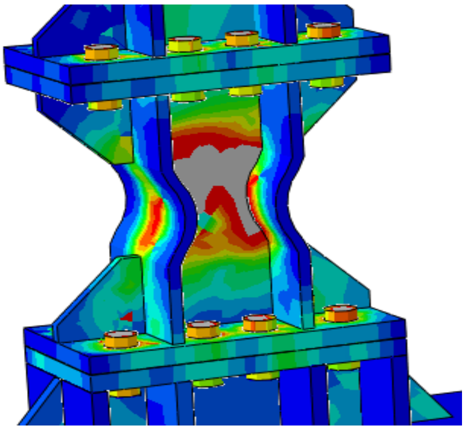

Fig. 13 Final von Mises stress distribution in the RDS-F Sample in the numerical model

models are presented in Table 4. It was observed that seven different sizes for the beam were considered, from IPB140 to IPB340. For each beam size, appropriate columns and specifications of the end plate were designed and selected (ANSI/AISC 358–16 2016). For each series, RBS, RBS-F, and RDS-F samples were constructed and a total of 21 numerical analyses were performed. The dimensions of the RDS sample were chosen so that the plastic section modulus would be equal to that of the RBS sample. Analyses continued up to 8% drift, similar to experimental conditions, and the moment-rotation hysteresis diagram was plotted for each sample. Since in tall structures, different beam and column dimensions were used, and the experimental test was performed for just one beam and column size, such extensive numerical analyses could provide a better comparison between the performances of the RDS and RBS connections.

Table 4 Specifications of numerical models

Models series	models name	Column section	Beam section	End plate thickness (mm)
1	RBS14, RBS-F14 and RDS-F14	IPB200	IPB140	18
2	RBS16, RBS-F16 and RDS-F16	IPB220	IPB160	20
3	RBS18, RBS-F18 and RDS-F18	IPB240	IPB180	25
4	RBS22, RBS-F22 and RDS-F22	IPB300	IPB220	25
5	RBS26, RBS-F26 and RDS-F26	IPB400	IPB260	25
6	RBS30, RBS-F30 and RDS-F30	IPB500	IPB300	30
7	RBS34, RBS-F34 and RDS-F34	IPB550	IPB340	30

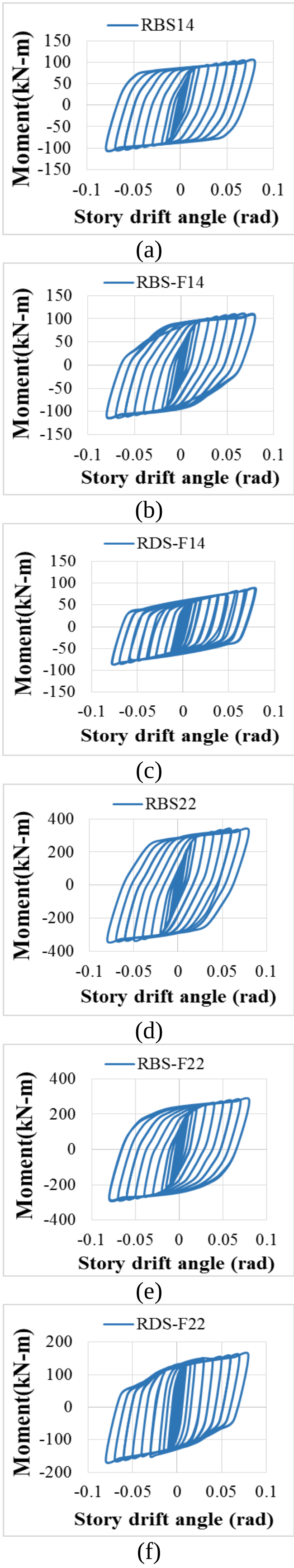

Fig. 14 Moment-drift diagram of numerical analysis of three models series 1 and 4

Fig. 14 shows the hysteresis diagram of the numerical models series 1 and 4 as examples. To investigate the seismic behavior of all the samples, their backbone and equivalent bilinear graphs were plotted. As a result, the stiffness, ductility, ultimate strength, and energy dissipation rates were obtained for the samples. Based on these features, the sample with the best performance could be selected.

4.1 Investigation of seismic properties in numerical models

For all the numerical models, the backbone diagram was plotted and the equivalent bilinear curve was fitted according to the criteria set forth in FEMA (FEMA- 440 2005). The backbone graph was plotted until the peak of the hysteresis curve and its declining portion was overlooked. The backbone diagram for models series 1 and 4 is presented in Fig. 15. Plotting the equivalent bilinear diagram should be done in such a way that the area under its curve is equal to the backbone graph. By plotting the equivalent bilinear diagram, the parameters of yield moment (My), yield drift (θy), maximum moment (Mm), and ultimate drift (θu) were determined. Furthermore, the effective stiffness (Ke) and ductility (μ) could be determined from Eqs. (1) and (2)

$$\mu = {}^{\theta_u}/_{\theta_y} \tag{1}$$

$$k_e = {}^{M_y}/_{\theta_y} \tag{2}$$

Ductility is one of the most important parameters in the design of the structure, which shows its ability to tolerate plastic deformations without significantly declining the strength. An accurate comparison of the seismic parameters of the experimental samples and numerical models is presented in Table 5. The values of θy, Ke, and μ in the experimental and numerical models differ by a maximum of 10%. Likewise, the values of θu, My, and Mm in the numerical and experimental samples vary by less than 5%. Therefore, the results of the numerical simulations are accurate and reliable.

Fig. 16 compares the ductility of numerical models. It was observed that the ductility in RBS and RBS-F samples were reduced by increasing the size of the sections. It has also been reported in a number of similar studies that increasing the size of the IPE section decreases the ductility of the connection [10]. This reduction rate was more present in RBS samples and less in RBS-F samples. The RDS-F sample had a much better performance in terms of ductility. Therefore, it was evident that the RDS-F had the highest degree of ductility among the samples. However, there was no significant change in ductility of this sample by changing the size of the cross-section.

The effective stiffness was the initial slope of the equivalent bilinear diagram, which depended on the yield strength and drift of the samples. As shown in Fig. 17, the effective stiffnesses of the RBS and RBS-F samples were

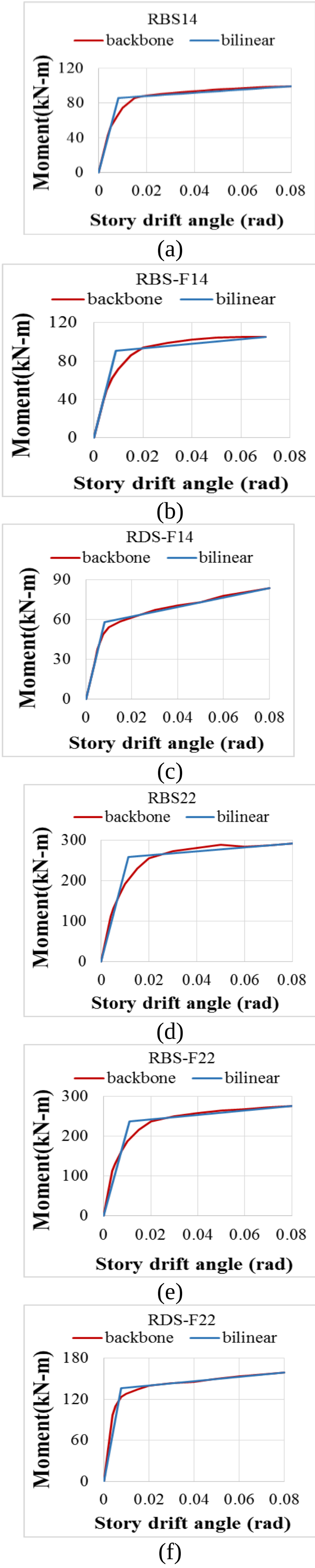

Fig. 15 Backbone and equivalent bilinear diagrams for models series 1 and 4

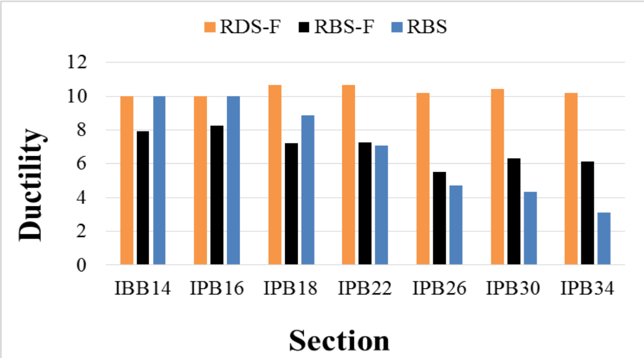

Fig. 16 Comparison among the ductility of RBS, RBS-F, and RDS-F specimens in numerical models

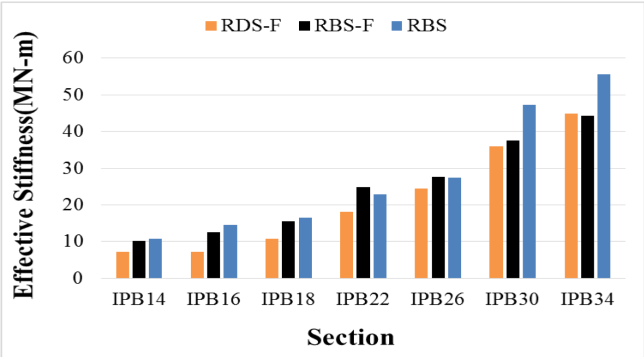

Fig. 17 Comparison of the effective stiffness of RBS, RBS-F, and RDS-F specimens in numerical models

Table 5 comparison of the seismic parameters in the experimental samples and numerical models

Sample	RBS Experimental	RBS Numerical	RBS-F Experimental	RBS-F Numerical	RDS-F Experimental	RDS-F Numerical
θ_y %	1.1	0.99	0.98	0.96	1.02	0.97
θ_u%	8	8	7	7	8	8
M_y (kN-m)	138.90	137.26	148.73	150.39	90.63	92.52
M_m (kN-m)	190.54	187.87	185.16	188.05	104.02	109.32
K_e (MN-m)	12.63	13.86	15.2	15.56	8.91	9.53
μ	7.27	8.08	7.12	7.24	7.87	8.24

slightly higher than that of the RDS-F specimens. Although not quite evident, the stiffness difference of the samples should be considered. The secant stiffness of the numerical samples of series 1, 4, and 7 were presented based on the backbone diagram in Fig. 18. It is noticeable that the stiffness drop was faster in the RDS-F sample.

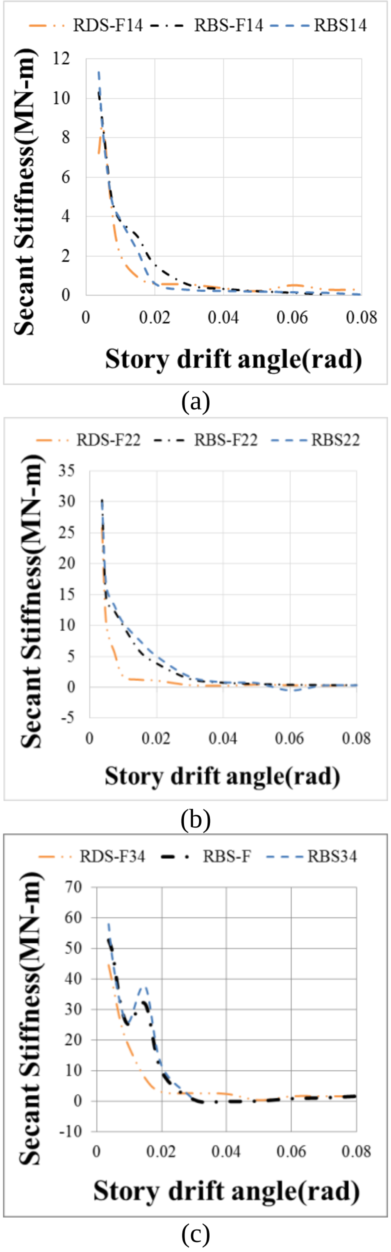

Fig. 18 Comparison of the secant stiffness of the numerical models of series 1, 4, and 7

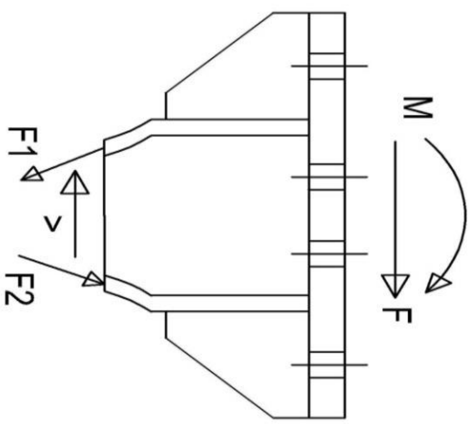

Fig. 19 Free body diagram in RDS-F sample

Although the RDS-F sample seemed to have a very good performance in terms of stability in hysteresis diagram and ductility, it encountered difficulty in terms of strength and stiffness. The main reason for this could be found in the connection geometry. Fig. 19 shows the free body diagram. It was clear that the pair of force acting on the flange increased the shear force in the section. Therefore, shear stress in the web was much higher than that of RBS and RBS-F specimens. Fig. 11(a) confirms this and shows that the failure of the RDS-F specimen in the laboratory initiated from the web. A comparison of Figs. 6 and 12 also shows the difference in how RBS and RDS sections yield. Therefore, the RDS cross-section needed to be strengthened in the web in order to increase stiffness and strength, as compared to the RBS samples, which will be discussed in the next section.

5. Modified RDS-F model

The RDS cross-section was highly ductile because of its geometry. Since the flange width ratio to the cross-sectional height was higher than that of the RBS samples, the lateral-tensional buckling and local buckling were expected to occur later. However, there was a significant increase in the shear stresses in the web when the plastic section modulus was the same as the RBS samples. Hence, its ultimate strength was lower. Therefore, there were two approaches to increasing the ultimate strength and stiffness in the RDS sample:

- Increasing the plastic modulus of the section than the RBS samples by decreasing R. R is the amount of depth reduction in the RDS section, as illustrated in Fig. 2(b).
- Increasing the thickness of the web

In this section, both approaches were employed simultaneously. Therefore, seven other numerical models were constructed for the RDS-FR sample. According to Fig. 2(b), it was observed that by reducing the amount of R, the plastic section modulus of these specimens was 20% higher than the RBS and RBS-F specimens. As shown in Table 6, the web thicknesses of the samples were also increased.

In Fig. 20, the final strength of all the 28 numerical samples is compared with each other. Clearly, the RDS-FR had a very good strength.

Table 6 Comparison of the web thickness and the R value in RDS-FR samples with RDS-F (dimensions in mm)

Beam Size	RDS-F		RDS-FR	
	Web Thickness	R	Web Thickness	R
IPB14	7	17.5	15	9
IPB16	8	23	17	14.5
IPB18	8	25	15	17
IPB22	9.5	29	20	16
IPB26	10	35	16	19.5
IPB30	11	40.5	20	22.5
IPB34	12	41	20	18.5

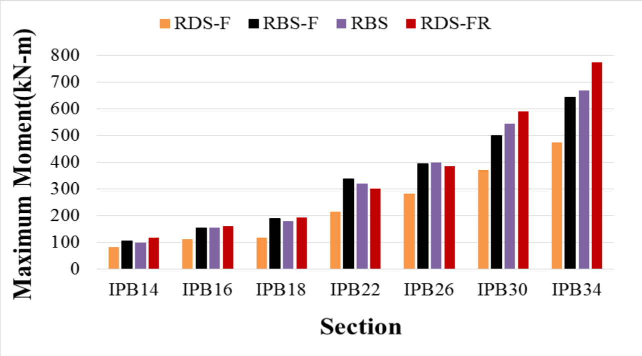

Fig. 20 Comparison of the ultimate strength of the numerical samples

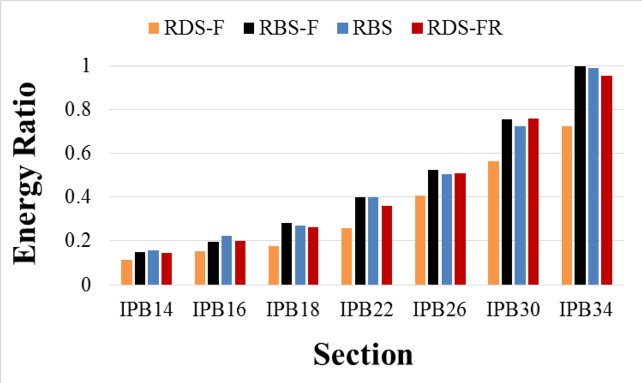

Fig. 21 Comparison of normalized cumulative energy dissipation of numerical samples

Further, the desired strength could be achieved by choosing the correct web thickness and the depth reduction in the fuse (R). In addition, the location of the plastic hinge is in the middle of the fuse in all of the RDS-FR models, and increasing the cross-sectional strength did not cause any plastic hinge movement. Therefore, there was no conflict with the philosophy of weakening the cross-section to protect the connection.

Energy dissipation was one of the most important seismic properties of each connection under the influence of cyclic loads that were obtained in each cycle based on the area under the moment-drift curve. Fig. 21 shows the amount of normalized cumulative energy dissipation for all numerical samples. It was clear that the energy dissipation of the RDS-F sample was less than the RBS and RBS-F samples because of the low ultimate strength. But the RDS-FR sample did not differ from the rest of the samples in terms of energy dissipation, and it also had a high energy dissipation capacity.

Fig. 22 shows the secant stiffness of the numerical samples of series 1, 4, and 7. It was noticeable that the stiffness drop of the RDS-FR sample occurred later compared to the other specimens and had a more proper performance.

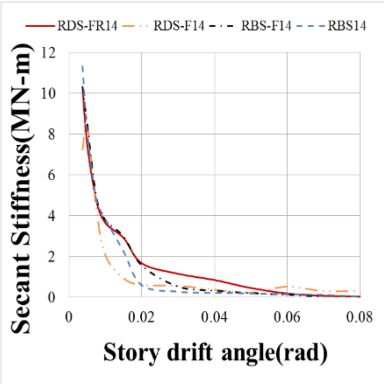

(a)

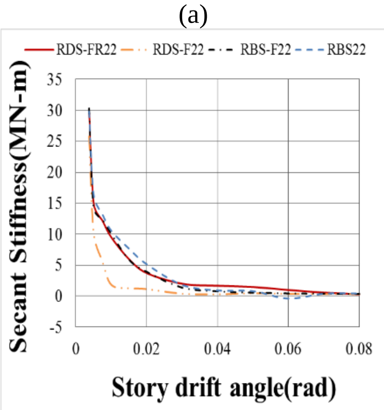

(b)

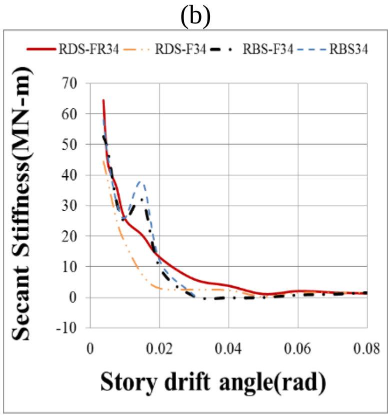

(c)

Fig. 22 Comparison of the secant stiffness of the numerical models of series 1, 4, and 7, taking into account the RDS-FR sample

The ductilities of each of the 28 numerical samples are compared in Fig. 23. Although, compared to the RDS-F sample, the ductility of the RDS-FR sample slightly decreased, it was still much larger than the RBS and RBS-F specimens. Thus, the RDS-FR sample was more ductile than the RBS and RBS-F specimens. It also maintained strength, stiffness, and energy dissipation. More importantly, possessing replaceable capability could help in having a high application in seismic areas with a high relative risk.

The results of this study revealed that in addition to having a stiffness and a strength on par with those of the RBS, the RDS-FR sample is also more ductile. Since the stiffness and strength of the RBS connection are ratified by

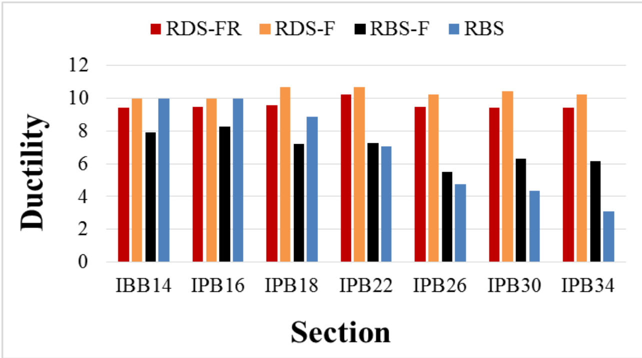

Fig. 23 Comparison of the ductility of each of the 28 numerical samples

different design codes, the RDS-FR sample, therefore, possesses the minimum stiffness and strength.

Due to secondary effects, the axial loads in the columns exert a considerable influence on the seismic behavior of the moment resisting frame. Therefore, to present design criteria for the RDS-FR sample, additional studies wherein the axial loads in the columns are accounted for need to be conducted. Also, the presence of stiffeners on both sides of the fuse and also the presence of the seating in the location where the fuse is connected to the column might present some problems when it comes to connecting the slab to the top of the beam. This, as well, needs further investigation.

6. Conclusions

In this paper, the possibility of using a reduced depth cross-section in a replaceable fuse was evaluated based on laboratory tests and numerical models. For this purpose, three full-scale samples were constructed, a sample of beam connections with reduced flange section and endplate (RBS), a sample with a fuse with reduced flange section (RBS-F), and a sample with a fuse with reduced depth section (RDS-F). The applied loading was quasi-static and cyclic, which continued until about the drift of 9%. Based on the three laboratory samples and more than 28 nonlinear finite element numerical models, the following results were obtained:

- The RBS-F sample had a performance similar to RBS sample. Therefore, it was preferred due to the purpose of replaceability after earthquakes.

- In the RBS and RBS-F samples, the ductility was reduced by increasing the beam size. While for the RDS-F, the ductility not only stayed constant by changing the size of the beam, but also significantly more than the other two samples.

- The RDS-F specimen with a plastic section modulus equivalent to the RBS-F sample had a lower ultimate strength and stiffness. The main reason behind this was the cross-sectional geometry with reduced depth.

- The modified RDS-F specimen with a greater thickness was proposed for the web as the final sample. This sample had a stiffness, ultimate strength, and energy dissipation around the RBS and RBS-F specimens.

However, its ductility is far higher.

Therefore, the use of the RDS-FR sample with very good seismic characteristics and the ability to replace was recommended in seismic areas. It has to be observed that the fuses are only replaceable when the damage sustained by the structure during an earthquake is concentrated in the fuses only. In the case of a strong earthquake, via structural components might be in need of retrofitting, which will render the replaceable fuse ineffective.

Acknowledgments

The authors would like to gratefully thank the structural research lab of the Islamic Azad University of Kermanshah and the 'NOVIN SAZE FIDER ZAGROSS Industrial Group' company.

References

ABAQUS/CAE User's Guide 6.13. 2016.

Akrami, V. and Erfani, S. (2015), "Effect of local web buckling on the cyclic behavior of reduced web beam sections (RWBS)", *Steel Compos. Struct.*, **18**(3), 641-657. https://doi.org/10.12989/scs.2015.18.3.641.

ANSI/AISC 358–16 (2016), Prequalified connections for special and intermediate steel moment frames for seismic applications, American Institute of Steel Construction; Chicago, Illinois, USA.

ASTM Standard A370-02 (2002), Standard test methods and definitions for mechanical testing of steel products, American Society for Testing and Materials; Philadelphia, PA.

DIN 18800, Teil 3: "Stahlbauten – Stabilitätsfälle, Plattenbeulen", Beuth Verlag GmbH, November 1990 DK 693.814.073.1.

Deylami, A. and Tabar, A.M. (2013), "Promotion of cyclic behavior of reduced beam section connections restraining beam web to local buckling", *Thin-Wall. Struct.*, **73**, 112-120.

Engelhardt, M.D. and Husain, A.S. (1993), "Cyclic-loading performance of welded flange-bolted web connection", *J. Struct. Eng.*, **119**(12), 3537-3550. https://doi.org/10.1061/(ASCE)0733-9445(1993)119:12(3537).

FEMA- 440 (2005), Improvement of nonlinear static seismic analysis procedures, Federal Emergency Management Agency; Redwood City.

FEMA-350 (2000), Recommended Seismic Design Provisions for New Moment Frame Buildings Report, Federal Emergency Management Agency; Washington DC.

Hassanien, S.H., Ramadan, H.M., Abdel-Salam, M.N. and Mourad, S.A. (2014), "Experimental study of prequalified status of flush end plate connections", *HBRC Journal*.

Hedayat, A.A. and Celikag, M. (2009), "Post-Northridge connection with modified beam end configuration to enhance strength and ductility", *J. Constr. Steel Res.*, **65**(7), 1413-1430. https://doi.org/10.1016/j.jcsr.2009.03.007.

ISO 898-1 (2009), mechanical properties of fasteners made of carbon steel and alloy steel —Part 1: , screws and studs with pacified property classes — coarse thread and fine pitch thread, International Organization for Standardization; Geneva, Switzerland.

Lee, C.H., Jeon, S.W., Kim, J.H. and Uang, C.M. (2005), "Effects of panel zone strength and beam web connection method on seismic performance of reduced beam section steel moment connections", *J. Struct. Eng.*, **131**(12), 1854-1865. https://doi.org/10.1061/(ASCE)0733-9445(2005)131:12(1854).

Lu, L., Xu, Y., Liu, J. and Lim, J. B. (2018), "Cyclic performance and design recommendations of a novel weak-axis reduced beam section connection", *Steel Compos. Struct.*, **27**(3), 337-353. https://doi.org/10.12989/scs.2018.27.3.337.

Mahin, S.A. (1998), "Lessons from damage to steel buildings during the Northridge earthquake", *Eng. Struct.*, **20**(4-6), 261-70. https://doi.org/10.1016/S0141-0296(97)00032-1.

Maleki, S. and Tabbakhha, M. (2012), "Numerical study of Slotted-Web–Reduced-Flange moment connection", *J. Constr. Steel Res.*, **69**(1), 1-7. https://doi.org/10.1016/j.jcsr.2011.06.003.

Miller, D.K. (1998), "Lessons learned from the Northridge earthquake", *Eng. Struct.*, **20**(4-6), 249-60. https://doi.org/10.1016/S0141-0296(97)00031-X.

Oh, K., Lee, K., Chen, L., Hong, S.B. and Yang, Y. (2015), "Seismic performance evaluation of weak axis column-tree moment connections with reduced beam section", *J. Constr. Steel Res.*, **105**, 28-38. https://doi.org/10.1016/j.jcsr.2014.10.005.

Rahnavard, R., Hassanipour, A. and Siahpolo, N. (2015), "Analytical study on new types of reduced beam section moment connections affecting cyclic behavior", *Case Studies in Struct. Eng.*, **3**, 33-51. https://doi.org/10.1016/j.csse.2015.03.001.

Roudsari, M.T., Abdollahi, F., Salimi, H., Azizi, S. and Khosravi, A.R. (2015), "The effect of stiffener on behavior of reduced beam section connections in steel moment-resisting frames", *Int. J. Steel Struct.*, **15**(4), 827-834.

Saleh, A., Zahrai, S.M. and Mirghaderi, S.R. (2016), "Experimental study on innovative tubular web RBS connections in steel MRFs with typical shallow beams", *Struct. Eng. Mech.*, **57**(5), 785-808. https://doi.org/10.12989/sem.2016.57.5.785.

Sofias, C.E., Kalfas, C.N. and Pachoumis, D.T. (2014), "Experimental and FEM analysis of reduced beam section moment endplate connections under cyclic loading", *Eng. Struct.*, **59**, 320-329. https://doi.org/10.1016/j.engstruct.2013.11.010.

Swati, A.K. and Gaurang, V. (2014), "Study of steel moment connection with and without reduced beam section", *Case Studies in Struct. Eng.*, **1**, 26-31. https://doi.org/10.1016/j.csse.2014.04.001.

Tahamouli Roudsari, M., Jamshidi K.H. and Mohebi Zangeneh, M. (2016), "Experimental and numerical investigation of IPE reduced beam sections with diagonal web stiffeners", *J. Earthq. Eng.*, 1-20. https://doi.org/10.1080/13632469.2016.1234422.

Tsavdaridis, K.D., Faghih, F. and Nikitas, N. (2014), "Assessment of perforated steel beam-to-column connections subjected to cyclic loading", *J. Earthq. Eng.*, **18**(8), 1302-1325. https://doi.org/10.1080/13632469.2014.935834.

Tsavdaridis, K.D. and Papadopoulos, T. (2016), "A FE parametric study of RWS beam-to-column bolted connections with cellular beams", *J. Constr. Steel Res.*, **116**, 92-113. https://doi.org/10.1016/j.jcsr.2015.08.046.

Wilkinson, S., Hurdman, G. and Crowther, A. (2006), "A moment resisting connection for earthquake resistant structures", *J. Constr. Steel Res.*, **62**(3), 295-302. https://doi.org/10.1016/j.jcsr.2005.07.011.

Zahrai, S.M., Mirghaderi, S.R. and Saleh, A. (2017a), "Tubular Web Reduced Beam Section (TW-RBS) connection, a numerical and experimental study and result comparison", *Steel Compos. Struct.*, **23**(5), 571-583. https://doi.org/10.12989/scs.2017.23.5.571.

Zahrai, S.M., Mirghaderi, S.R. and Saleh, A. (2017b), "Increasing plastic hinge length using two pipes in a proposed web reduced beam section, an experimental and numerical study", *Steel Compos. Struct.*, **23**(4), 421-433. https://doi.org/10.12989/scs.2017.23.4.421.

Zareia, A., Vaghefi, M. and Fiouz, A.R. (2016), “Numerical investigation seismic performance of rigid skewed beam-to-column connection with reduced beam section”, *Struct. Eng. Mech.*, **57**(3), 507-528. https://doi.org/10.12989/sem.2016.57.3.507.

BU